

# PHOTOCONDUCTIVE SWITCH CHARACTERIZATION BY MEANS OF DEEP LEVEL SPECTROSCOPY

R.P. Brinkmann<sup>a,b</sup>, T. Tessnow<sup>b</sup>, K.H. Schoenbach<sup>b</sup>, R.A. Roush<sup>c</sup>

a: Siemens AC, ZFE BT ACM 31, D-81730 München

b: PERI, Old Dominion University, Norfolk, VA 23529

c: Naval Surface Warfare Center, Dahlgren, VA 22448

## Abstract

DLTS (deep level transient spectroscopy), PICTS (photo-induced current transient spectroscopy), and EBICTS (electron-beam induced current transient spectroscopy) are experimental techniques to determine the deep level spectrum of non-ideal semiconductors. These methods operate by externally exciting a sample of the material, and then monitoring the time constants of the subsequent return to equilibrium. We analyze the conventional ("rate window") method of evaluating the experimental data obtained by these techniques, and find it wanting in many respects. A new method (termed "spectral analysis") is then presented which is superior both in terms of accuracy and resolution, and which also makes the deep level spectroscopy techniques more suited for numerical evaluation.

## Introduction

The performance of radiation (i.e., laser or electron-beam) controlled solid state switches depends strongly on the properties of the employed semiconductor material. Recent investigations have shown that not only the ideal features of the material are of importance, but also the non-ideal characteristics related to the nature and the concentration of impurities and other crystal flaws. By inducing additional discrete states (so-called deep levels or traps) into the band structure of the semiconductor, one can drastically influence the critical performance measures like efficiency, hold-off voltage, and recovery time [1], and can even open the possibility of completely new switch concepts [2].

In this situation, both the analysis and the design of solid state switches require reliable information about the location, the cross sections, and the number densities of the deep levels in the employed material. Several experimental methods have been designed to obtain this information, the most widely used are known by their acronyms as DLTS (deep level transient spectroscopy) [3], PICTS (photo-induced current transient spectroscopy) [4], and EBICTS (electron-beam induced current transient spectroscopy) [5]. The principles of these methods are very similar, they operate by externally exciting a sample of the material, and analyzing the time constants of the subsequent return to equilibrium as a function of the temperature.

The last two methods are particularly similar, for they both use irradiation as means of excitation, and monitor the sample conductance as a measure for the excitation. Both methods are especially suited for the analysis of semi-insulating semiconductor materials which form the basis of all optically activated switch concepts. The principle set-up of the methods is schematically depicted in Fig. 1.

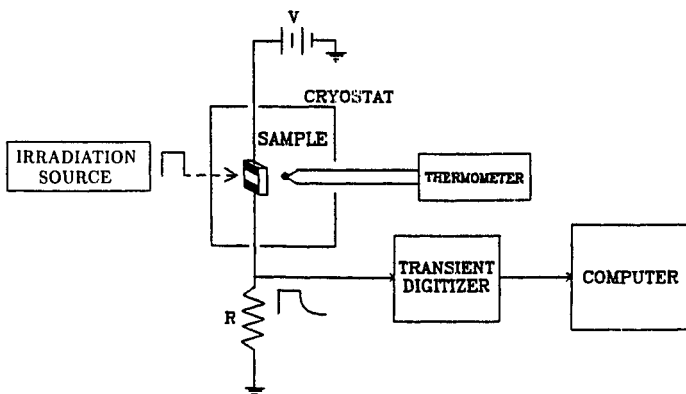


Fig. 1: Principle set-up for deep-level spectroscopy, with "irradiation source" denoting either a laser (PICTS) or an electron-beam (EBICTS).

A sample of the material under consideration is furnished with two coplanar Ohmic contacts of a few mm spacing, and then mounted on a thermally isolated holder within an electrically grounded cryostat. The temperature of the cryostat can be adjusted in the range from 77 K (liquid nitrogen cooling) to 400 K (electrical heating), it can be directly monitored by means of a T-type thermo element. Through an opening in the cryostat, the device is subjected to an irradiation pulse (laser light in the case of PICTS, energetic electrons in the case of EBICTS) which brings it into a state of high electronic excitation; the increased conductivity and its subsequent return to equilibrium can be monitored by means of an external voltage source and a current viewing resistor. The signal is then recorded by a transient digitizer and finally stored as a numerical computer file.

The basic assumption of deep level spectroscopy is that the time constants which govern the return to equilibrium contain essential information on the level spectrum of the material. In general, the dynamics can be quite complicated to analyze, let us thus focus on a situation where only one isolated electron trap of total concentration  $N$  is active in a material with electron lifetime  $\tau$ . In this case, the carrier kinetics can be described in terms of two rate equations for  $n$  and  $n_T$ , the density of the electrons in the valence band and in the trap, respectively,

$$\frac{dn}{dt} = K(e_n n_T - n(N - n_T)) - \frac{n}{\tau}, \quad (1)$$

$$\frac{dn_T}{dt} = K(n(N - n_T) - e_n n_T). \quad (2)$$

$K$  and  $e_n$  describe the constants of electron capture and thermal emission of the trap, they depend on the cross section  $\sigma$ , the ionization energy  $\Delta E$  and the temperature  $T$ . (Furthermore,  $g$  is the statistical weight of the level,  $m$  the effective electron mass,  $k$  and  $h$  denote Boltzmann's and Planck's constant, respectively.)

$$K = \sigma \sqrt{\frac{8kT}{\pi m}}, \quad (3)$$

$$e_n = \frac{2}{g} \left( \frac{mkT}{2\pi\hbar^2} \right)^{\frac{3}{2}} \exp\left(-\frac{\Delta E}{kT}\right). \quad (4)$$

To describe the recovery, the equations can be even more simplified: The term  $\sim n(N - n_T)$  representing back-trapping becomes negligible, and the term  $\frac{dn}{dt}$  on the left of (1) can be dropped (under the assumption that  $KN \ll \tau^{-1}$ , i.e., that the trap is dominated by other channels of electron recombination.) We can then solve the equations explicitly; assuming that the trap is filled at  $t = 0$ , the electron density is

$$n(t) = \lambda \tau N \exp(-\lambda t). \quad (5)$$

(The sample current  $i$  is proportional to this quantity, times a factor which depends on the geometry of the sample, the applied voltage, and on the specific mobility of the carriers.) The time constant  $\lambda$  equals  $Ke_n$ , in terms of the cross section and the energy level of the trap it is

$$\lambda = \frac{2\sigma mk^2}{\pi^2 g \hbar^3} T^2 \exp\left(-\frac{\Delta E}{kT}\right). \quad (6)$$

Under the assumption that the deep level parameters contain no implicit dependence on the temperature  $T$ , we can plot  $\lambda/T^2$  logarithmically and obtain a linear function in  $1/T$ , the so-called Arrhenius plot. The slope of this function is proportional to the ionization energy of the deep level  $\Delta E$ , and the absolute term contains the cross section  $\sigma$ .

So far, the evaluation of the data obtained by deep level spectroscopy seems completely straightforward. We have, however, tacitly glossed over a problem that is by no means trivial: How can one determine the rate constants  $\lambda$  from the actually observed current  $i(t)$ , in particular when there is a chance of more than one trap being active in the data?

Report Documentation Page			Form Approved OMB No. 0704-0188		
Public reporting burden for the collection of information is estimated to average 1 hour per response, including the time for reviewing instructions, searching existing data sources, gathering and maintaining the data needed, and completing and reviewing the collection of information. Send comments regarding this burden estimate or any other aspect of this collection of information, including suggestions for reducing this burden, to Washington Headquarters Services, Directorate for Information Operations and Reports, 1215 Jefferson Davis Highway, Suite 1204, Arlington VA 22202-4302. Respondents should be aware that notwithstanding any other provision of law, no person shall be subject to a penalty for failing to comply with a collection of information if it does not display a currently valid OMB control number.					
1. REPORT DATE <b>JUN 1993</b>		2. REPORT TYPE <b>N/A</b>		3. DATES COVERED <b>-</b>	
4. TITLE AND SUBTITLE <b>Photoconductive Switch Characterization By Means Of Deep Level Spectroscopy</b>				5a. CONTRACT NUMBER	
				5b. GRANT NUMBER	
				5c. PROGRAM ELEMENT NUMBER	
6. AUTHOR(S)				5d. PROJECT NUMBER	
				5e. TASK NUMBER	
				5f. WORK UNIT NUMBER	
7. PERFORMING ORGANIZATION NAME(S) AND ADDRESS(ES) <b>Siemens AC, ZFE BT ACM 31, D-81730 Miinchen</b>				8. PERFORMING ORGANIZATION REPORT NUMBER	
9. SPONSORING/MONITORING AGENCY NAME(S) AND ADDRESS(ES)				10. SPONSOR/MONITOR'S ACRONYM(S)	
				11. SPONSOR/MONITOR'S REPORT NUMBER(S)	
12. DISTRIBUTION/AVAILABILITY STATEMENT <b>Approved for public release, distribution unlimited</b>					
13. SUPPLEMENTARY NOTES <b>See also ADM002371. 2013 IEEE Pulsed Power Conference, Digest of Technical Papers 1976-2013, and Abstracts of the 2013 IEEE International Conference on Plasma Science. Held in San Francisco, CA on 16-21 June 2013. U.S. Government or Federal Purpose Rights License.</b>					
14. ABSTRACT <b>DLTS (deep level transient spectroscopy), PICTS (photo-induced current transient spectroscopy), and EBICTS (electron-beam induced current transient spectroscopy) are experimental techniques to determine the deep level spectrum of non-ideal semiconductors. These methods operate by externally exciting a sample of the material, and then monitoring the time constants of the subsequent return to equilibrium. We analyze the conventional ("rate window") method of evaluating the experimental data obtained by these techniques, and find it wanting in many respects. A new method (termed "spectral analysis") is then presented which is superior both in terms of accuracy and resolution, and which also makes the deep level spectroscopy techniques more suited for numerical evaluation.</b>					
15. SUBJECT TERMS					
16. SECURITY CLASSIFICATION OF:			17. LIMITATION OF ABSTRACT <b>SAR</b>	18. NUMBER OF PAGES <b>4</b>	19a. NAME OF RESPONSIBLE PERSON
a. REPORT <b>unclassified</b>	b. ABSTRACT <b>unclassified</b>	c. THIS PAGE <b>unclassified</b>			

The traditional procedure of evaluating deep levels spectroscopy data is known as the rate-window technique [6]. The method is based on the observation that the difference of the response current at two time points,  $\Delta i = i(t_1) - i(t_2)$ , is unequal from zero only when the time constant lies within a certain window (see Fig. 2). Indeed, for a single exponential mode of the form  $i(t) = A \exp(-\lambda t)$  the difference as a function of  $\lambda$  has a maximum at

$$\lambda = \frac{\ln(t_2/t_1)}{t_2 - t_1}. \quad (7)$$

Correspondingly, if the temperature of the sample is scanned through a certain interval, a peak in the plot of  $\Delta i$  over  $T$  marks the passing of time constant though the "rate window".

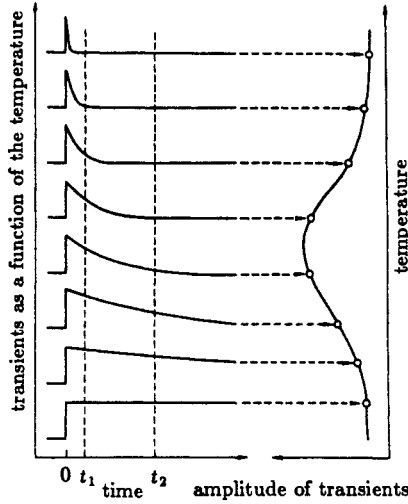


Fig. 2: Signal difference  $\Delta i$  as a function of the time constant of a single-mode signal (itself being a function of the sample temperature).

To analyze the sensitivity and the resolution of the rate window technique, it is advantageous to switch to a different point of view. Instead of modifying the rate constants embodied in  $i(t)$  (by changing the temperature of the sample), we concentrate on a single response curve and evaluate  $\Delta i$  as a function of the window interval  $[t_1, t_2]$ . Assuming that the ratio  $t_1/t_2 = \eta$  is constant ( $\equiv 0.5$  in the following examples), and introducing a new independent variable  $\lambda$  via relation (7), we can express the signal difference as

$$\Delta i(\lambda) = i\left(\frac{\eta \ln(1/\eta)}{(1-\eta)\lambda}\right) - i\left(\frac{\ln(1/\eta)}{(1-\eta)\lambda}\right). \quad (8)$$

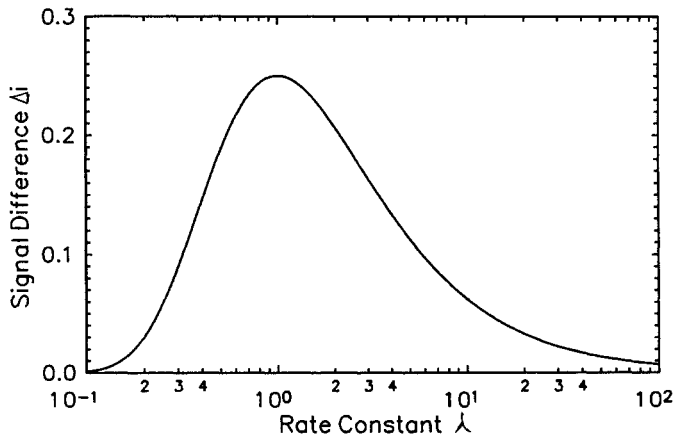


Fig. 3: Signal difference  $\Delta i$  for a single-mode response  $i(t) = \exp(-t)$ , as function of the spectral parameter  $\lambda$  (an independent variable).

We infer from the form of expression (8) that a change of the temporal scale of the input signal,  $t \rightarrow at$ , corresponds to a transformation  $\lambda \rightarrow \lambda/a$  in the function  $\Delta(\lambda)$ . It is thus natural to plot the signal difference in logarithmic coordinates (where re-scaling is equivalent to a lateral shift); we will refer to such a plot of  $\Delta i$  over  $\ln(\lambda)$  as the "rate window spectrum" of  $i(t)$ . For a single-mode response  $i(t) = I \exp(-\lambda t)$ , the spectrum has a single peak located at  $\bar{\lambda}$  (the rate constant of the signal), it falls to zero both for  $\lambda \rightarrow 0$  and  $\lambda \rightarrow \infty$ . Fig. 3 illustrates this for the normalized case  $I = \lambda = 1$ , where the spectrum follows (for  $\eta = 0.5$ ) the explicit form

$$\Delta i(\lambda) = 2^{-\frac{1}{\lambda}} (1 - 2^{-\frac{1}{\lambda}}). \quad (9)$$

Because of the linearity of definition (8), the spectrum of a sum of exponential modes consists of the superposition of the corresponding single-mode responses. Unfortunately, however, the width of the peaks is relatively broad, and they can be resolved individually only when the time constants are sufficiently separated from each other. Figs. 4 and 5 demonstrate this effect for two modes of the same amplitude, separated by factors  $\bar{\lambda}_2/\bar{\lambda}_1$  of 5, 10, 100 and 1000, respectively.

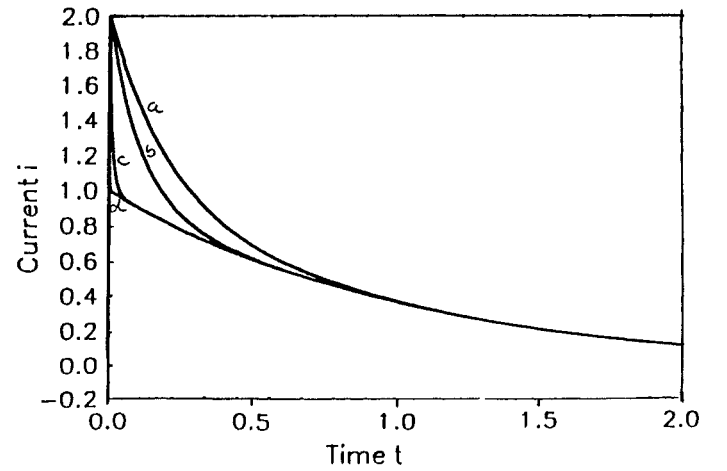


Fig. 4: A signal  $i(t)$  consisting of two superimposed mode of equal amplitude ( $A = 1$ ), with  $\lambda_1 = 1$  and  $\lambda_2 = 5, 10, 100, 1000$ , respectively.

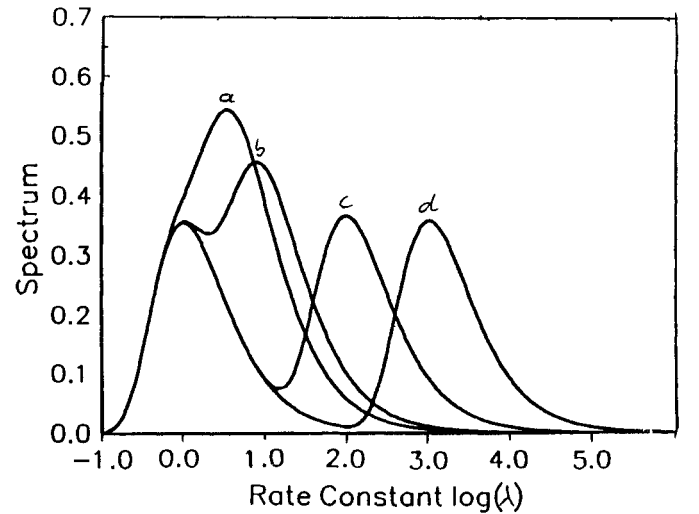


Fig. 5: The rate window spectra for the four different cases of Fig. 4.

The figures demonstrate that different modes can only be resolved when the separation between the time constants exceeds a factor of ten. For traps with identical cross sections, this corresponds to an energy resolution of not better than  $2kT$  (about 50 meV at room temperature). Clearly, it is desirable to do better than that.

## Spectral Analysis

Our alternative evaluation method “spectral analysis” is motivated by the form of the data collected in deep level spectroscopy experiments. Namely, what one actually obtains from a set-up like the one depicted in figure 1 is not just two data points  $i_1$  and  $i_2$  (nor a continuous curve  $i(t)$  as assumed for our analysis), but a discrete set of digitally recorded values  $i_k$  at equally spaced timepoints  $t_k = (k-1)\Delta t$ ,  $k = 1 \dots N$ . Taking into account that the measurement will also be subject to some superimposed noise, the data (of a signal with  $M$  modes) has the form

$$i_k = \sum_{\mu=1}^M I_{\mu} \exp(-\lambda_{\mu} t_k) + \delta i_k. \quad (10)$$

The task of any evaluation method is to invert this relation, i.e., to determine the  $2M$  mode parameters from the  $N$  measured data  $i_k$ . Obviously, because of the super-imposed noise, there cannot be an exact solution to that problem, the best we can hope for is an “optimal choice” based on some appropriate statistical procedure. The first approach that comes to mind is a least-square fit, with the  $I_{\mu}$  and  $\lambda_{\mu}$  chosen such that the total squared deviation assumes its minimum:

$$\Delta^2 = \sum_{k=1}^N \left( \sum_{\mu=1}^M I_{\mu} \exp(-\lambda_{\mu} t_k) - i_k \right)^2 \stackrel{!}{=} \text{Min}. \quad (11)$$

For two reasons, however, this is not the optimal approach. First, the system of equations derived from (11) is nonlinear (and ill-conditioned), so that a direct solution is difficult to obtain. And secondly, the number of modes present in the signal is not known *a priori*, so that  $M$  must be treated as an additional unknown. Both difficulties can be overcome if we allow not only for discrete modes, but also for a continuous mode distribution (a “spectrum”)  $I(\lambda)$  by making the ansatz

$$i_k = \int_0^{\infty} I(\lambda) \exp(-\lambda t_k) d\lambda + \delta i_k. \quad (12)$$

Clearly, it is not possible to calculate the spectrum directly by means of a least-square fit; the knowledge of a finite number of data points ( $i_k$ ) is not sufficient to completely determine a continuous function ( $I$ ). Indeed, there is an infinite number of possible spectra that represent the data equally well. Most of these functions, however, are highly irregular, i.e., contain strong (even discontinuous) fluctuations and values in the negative range. We can suppress these unphysical solutions – which have their origin in the fact that the inverse of the integral-operator in (12) is unbounded and hence not continuous – with the help of a suitable regularization of the problem. We proceed as follows:

Instead of searching for the “best” fit, we specify a certain quality level, i.e., a maximum quadratic deviation  $\Delta^2$ , and then determine the “most physical” spectrum that meets the requirement. In other words, we search for the (in logarithmic scale) smoothest spectrum

$$\|I\| = \int_0^{\infty} I^2(\lambda) \frac{d\lambda}{\lambda} \stackrel{!}{=} \text{Min} \quad (13)$$

among all positive trial functions

$$I(\lambda) \geq 0, \quad \lambda \in (0, \infty), \quad (14)$$

which sufficiently represent the data

$$\sum_{k=1}^N \left( \int_0^{\infty} I(\lambda) \exp(-\lambda t_k) d\lambda - i_k \right)^2 \leq \Delta^2. \quad (15)$$

Clearly, this task is equivalent to a variational problem with constraints, represented by the Lagrangian function

$$\begin{aligned} \mathcal{L} = & \frac{1}{2} \int_0^{\infty} I^2(\lambda) \frac{d\lambda}{\lambda} + \int_0^{\infty} V(\lambda) I(\lambda) d\lambda \\ & + \frac{1}{2} \Lambda \left[ \sum_{k=1}^N \left( \int_0^{\infty} I(\lambda) \exp(-\lambda t_k) d\lambda - i_k \right)^2 - \Delta^2 \right], \end{aligned} \quad (16)$$

where the function  $V(\lambda)$  ensures the positivity of the solution and the parameter  $\Lambda \in [0, \infty)$  takes the data condition into account.

Standard variational calculus allows us to uniquely determine the minimizing spectrum as

$$I(\lambda) = \begin{cases} \sum_{k=1}^N J_k \lambda \exp(-\lambda t_k) & \lambda \in S \\ 0 & \lambda \notin S, \end{cases} \quad (17)$$

where the  $J_k$  denote the solution of the matrix equation

$$\frac{1}{\Lambda} J_k + \sum_{l=1}^N M_{kl} J_l = i_k \quad (18)$$

with  $M$  given as

$$M_{kl} = \int_S \lambda \exp(-\lambda(t_k + t_l)) d\lambda. \quad (19)$$

In these equations, the support  $S$  is defined as that subset of  $(0, \infty)$  where the exponential polynomial is greater than or equal to zero,

$$S = \left\{ \lambda \in (0, \infty) \left| \sum_{k=1}^N J_k \lambda \exp(-\lambda t_k) \geq 0 \right. \right\}. \quad (20)$$

For each set of current data  $i_k$ , equations (17) to (20) determine a family of spectra  $I(\lambda)$ , parametrized by the Lagrangian multiplier  $\Lambda$ . For  $\Lambda = 0$ , the “smoothest” solution is chosen, namely the one identical to zero, and no attention is paid to the data constraint (15). For greater values of  $\Lambda$ , the fit becomes increasingly better, and correspondingly the spectrum becomes more and more peaked; generally, it holds

$$\frac{d}{d\Lambda} \|I\|^2 > 0, \quad (21)$$

$$\frac{d}{d\Lambda} \Delta^2 < 0. \quad (22)$$

In the limit  $\Lambda \rightarrow \infty$ , the spectrum converges to a sum of  $\delta$ -functions, and one can recover the “optimal choice” for the mode parameters of ansatz (10): Denoting by  $S_{\mu}$  ( $\mu = 1 \dots M$ ) the partition of the support into its compact subsets, the relations are

$$\lambda_{\mu} = \lim_{\Lambda \rightarrow \infty} \int_{S_{\mu}} d\lambda, \quad (23)$$

$$I_{\mu} = \lim_{\Lambda \rightarrow \infty} \int_{S_{\mu}} I(\lambda) d\lambda. \quad (24)$$

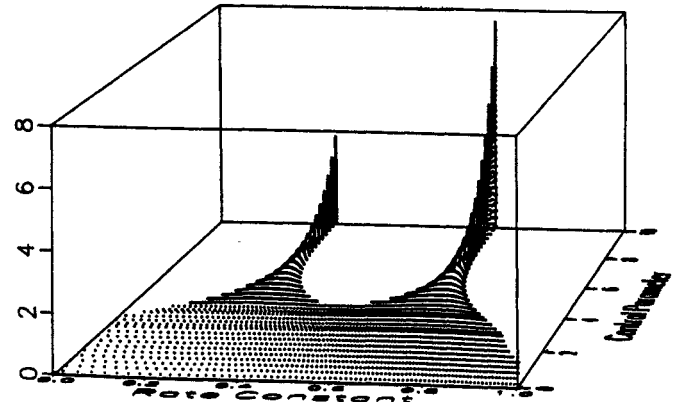


Fig. 6: Family of spectra  $I(\lambda)$  for the current data given in Fig. 7, parametrized by the Lagrangian multiplier  $\Lambda$  ( $0 \leq \lambda \leq 1, 1 \leq \Lambda \leq 10^{10}$ ).

It is interesting to note that this behavior (illustrated by Fig. 6) is actually the basis of our numerical solution strategy: While, for any given finite value, the spectral equations are rather difficult to solve, we found it very satisfactory to start at  $\Lambda = 0$  and follow the trajectory of the  $J_k(\Lambda)$  through solution space (using Newton’s scheme).

Having outlined the principles both of the rate window method and of spectral analysis, we now proceed to compare the techniques directly. First, it is clear that our new approach requires a considerably increased mathematical and numerical effort compared to the rate window method; among other things it requires the repeated iterative solution of a coupled set of  $N$  nonlinear equations, with each iteration involving an eigenvalue/eigenvector search and the determination of all positive real zeros of a high-order exponential polynomial. To demonstrate that this increased effort is really justified, let us apply both schemes to a set of constructed data with known characteristics. Fig. 7 shows such a set of 50 data points, representing a two-mode spectroscopy signal superimposed with some Gaussian noise reflecting measurement errors. Explicitly, we assumed a form

$$i_k = 0.4 \exp(-2t_k) + 1.5 \exp(-5t_k) + \delta i_k, \quad (25)$$

with  $t_k$  equally spaced at intervals of  $\Delta t = 0.1$ ,  $t_k = 0.1(k-1) + 0.05$ , and  $\delta i_k$  drawn from a normal distribution  $n(0, 0.05)$  with zero mean and 0.05 standard deviation ( $\equiv$  relative error of about 2.5%).

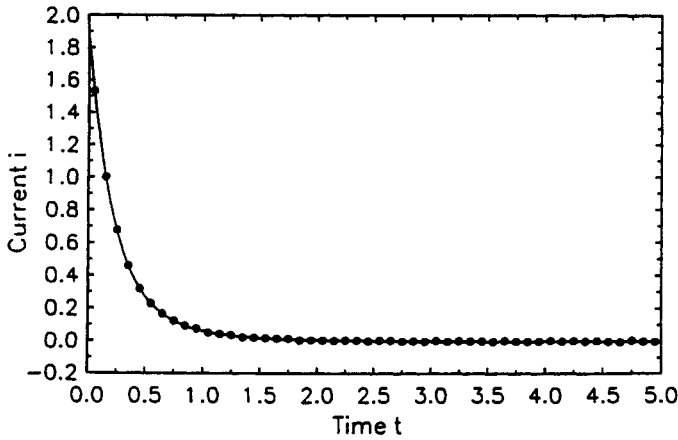


Fig. 7: Constructed spectroscopy signal as basis of a method comparison, consisting of two modes ( $\bar{\lambda}_1 = 2$ ,  $\bar{\lambda}_2 = 5$ ) with superimposed noise.

Let us first consider the results of the original rate window method. Fig. 8 shows the spectrum  $\Delta i(\lambda)$  as defined in equation (8), plotted logarithmically in three decades ranging from  $\lambda = 0.1$  to  $\lambda = 100$ . As expected (because  $\bar{\lambda}_2/\bar{\lambda}_1 = 2.5$  is smaller than the minimum resolution of about 10), it is not possible to separate the two modes present in the signal. Instead, the spectrum is represented as one single peak with the maximum located  $\bar{\lambda} \approx 4.5$ . (Graphical evaluation.)

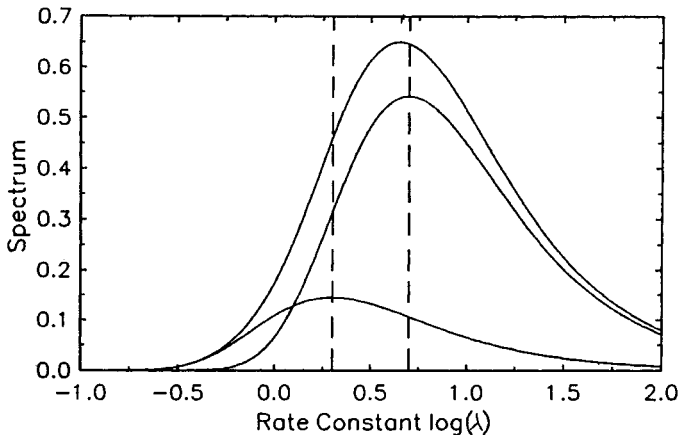


Fig. 8: Rate window  $\Delta i$  spectrum for the two-mode signal displayed in Fig. 7, with the separate single-mode spectra shown for comparison.

Now we turn to analyzing the results of the spectral analysis method. Fig. 9 depicts the spectrum  $I(\lambda)$  in the range of 1 to 10, evaluated for  $\Lambda = 10^{10}$ . (Note that the interval spans only one decade, as opposed to three in Fig. 8.) The spectrum clearly resolves the two modes present in the signal; both the rate constants  $\lambda$  and the amplitudes  $I$  are estimated with reasonable accuracy. Further investigations confirmed that the error of 5-10% is directly related to the superimposed noise, for  $\delta i_k \equiv 0$  we were able to determine the constants up to an accuracy of  $10^{-6}$ .

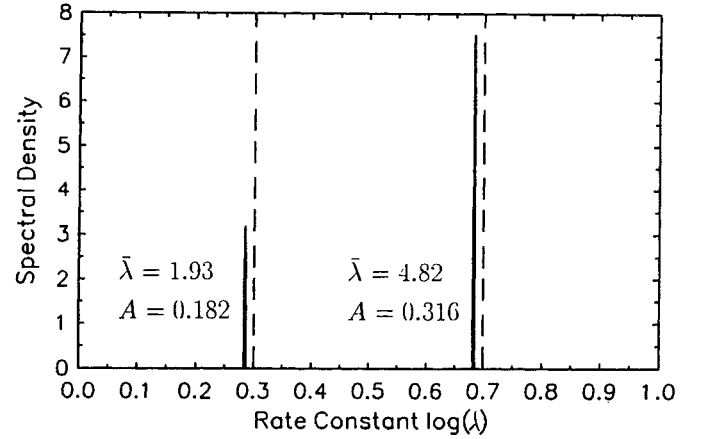


Fig. 9: Spectrum  $I(\lambda)$  of the spectral analysis method, with  $\Lambda = 10^{10}$ .

A comparison of the two spectra clearly shows the superiority of the spectral analysis technique, both in terms of resolution and accuracy. Extended numerical experiments have shown that there are no principle bounds in this respect, the achievable quality is only limited by superimposed noise of the input data (and the accuracy of the employed floating point arithmetic). At a noise level of 2.5%, rate constants which differed by less than 1.5 could easily be resolved. This corresponds to an energy resolution of better than 10 meV at room temperature, an 500% improvement over the rate window method.

An additional advantage of the new technique is that it is also better adapted to the experimental set-up depicted in Fig. 1: The actually collected data are a finite number (typically 1024) of values  $i_k$  sampled at equidistant times  $t_k$ ; just as required by the spectral analysis technique. To use only two of these data points (as in the traditional rate window method) would correspond to wasting the bulk of the already acquired information; to exploit the knowledge of the complete function  $i(t)$  (as we did in our analysis) would require the use of potentially unstable methods of extrapolation.

Much further effort is required before our technique can replace the rate window method as the standard tool of deep level spectroscopy: Tests must be implemented to decide whether the data can be reasonably represented by an exponential sum in the first place. A statistical analysis of the relation between the quality of the input and the confidence limits of the output is needed, and an interactive user interface must be designed to allow convenient manipulation and evaluation of large amounts of data. Nonetheless, we believe that the demonstrated advantages of the new method will make this effort worthwhile.

### References

- [1] R.P. Brinkmann, K.H. Schoenbach, D.C. Stoudt, V.K. Lakdawala, and M.K. Kennedy, *IEEE Trans. Electron Devices*, **38**, 701 (1991).
- [2] K.H. Schoenbach, V.K. Lakdawala, R.F.K. Germer, and S.T. Ko, *J. Appl. Phys.*, **63**, 2460, 1988.
- [3] D.V. Lang and R.A. Logan, *J. Appl. Phys.*, **47**, 1533, (1976).
- [4] D.K. Schröder, *Semiconductor Material and Device Characterization*, New York (1990).
- [5] T. Tesson, K.H. Schoenbach, R.A. Roush, R.P. Brinkmann, L. Thomas, and R.K.F. Germer, in *Proceedings 20. International Symposium on GaAs and Related Compounds*, Freiburg, 1993.
- [6] D.V. Lang, in *Thermally Stimulated Relaxation in Solids*, P. Bräunlich (ed.), Berlin, 1979, p. 93.